

# DYNAMIC RESPONSE IMPROVEMENT OF DOUBLY FED INDUCTION GENERATOR-BASED WIND FARM USING FUZZY LOGIC CONTROLLER

Hany M. Hasanien — Essam A. Al-Ammar \*

Doubly fed induction generator (DFIG) based wind farm is today the most widely used concept. This paper presents dynamic response enhancement of DFIG based wind farm under remote fault conditions using the fuzzy logic controller. The goal of the work is to improve the dynamic response of DFIG based wind farm during and after the clearance of fault using the proposed controller. The stability of wind farm during and after the clearance of fault is investigated. The effectiveness of the fuzzy logic controller is then compared with that of a PI controller. The validity of the controllers in restoring the wind farms normal operation after the clearance of fault is illustrated by the simulation results which are carried out using MATLAB/SIMULINK. Simulation results are analyzed under different fault conditions.

**Key words:** doubly fed induction generator, wind farm, remote fault, fuzzy logic controller

## 1 INTRODUCTION

As a result of conventional energy sources consumption and increasing environmental concern, great efforts have been done to produce electricity from renewable sources, such as wind energy sources. Institutional support on wind energy sources, together with the wind energy potential and improvement of wind energy conversion technology, have led to a fast development of wind power generation in recent years [1–3]. Proposals for wind developments in the hundreds of MWs are currently being considered. Interconnection of these developments into the existing utility grid poses a great number of challenges [4].

The doubly fed induction generator (DFIG) based wind turbines are nowadays more widely used in large wind farms. The main reasons for the increasing number of DFIGs connected to the electric grid are low converter power rating and ability to supply power at constant voltage and frequency while the rotor speed varies [5]. The DFIG concept also provides possibility to control the overall system power factor.

In the DFIG, the stator is directly connected to the grid and the three phase rotor windings are supplied from a pulse width modulated (PWM) frequency converter via slip rings as shown in Fig. 1. The control performance is excellent in normal grid conditions allowing active and reactive power changes in the range of few milliseconds [6].

In low penetration level of wind power, Wind farms mostly do not take part in voltage and frequency control and if a fault occurs, the wind farms are disconnected and reconnected when normal operation has been resumed.

Thus, the frequency and voltage are maintained by controlling the large power plants as would have been the case without any wind turbines present [7].

However, a tendency to increase the amount of electricity generated from wind is observed. Therefore, many researches nowadays trend to study the dynamic response of wind farms during and after the clearance of the fault without disconnection of the wind farms [8–10]. This represents a challenge of the DFIG based wind farms controllers in order to make the system stable and recover it again to its normal operation condition.

Due to their simple structure and robust performance, proportional-integral (PI) controllers are the most common controllers used to generate the signal that controls the DFIG. However, the success of the PI controller, and consequently the performance of the DFIG depend on the appropriate choice of the PI gains. Fine tuning the PI gains to optimize performance takes a lot of time, and it is cumbersome especially when the system is nonlinear. Fuzzy logic controller (FLC) provides another way of thinking to control a nonlinear process based on human experience. This may be considered as a heuristic approach that can improve the performance of closed loop systems [11].

In this paper, a detailed model for representation DFIG based wind farm in power system dynamics simulations is presented. MATLAB/SIMULINK dynamic software program is used for this study [12]. This paper presents dynamic response enhancement of DFIG based wind farm under remote fault conditions using the fuzzy logic controller. The goal of the work is to improve the dynamic response of DFIG based wind farm during and after the clearance of fault using the proposed controller. The stability of wind farm during and after the clearance

\* Saudi Aramco Chair in Electrical Power, Electrical Engineering Department, College of Engineering, King Saud University, Riyadh, 11421, P.O. Box 800, Saudi Arabia, hanyhasanien@yahoo.ca

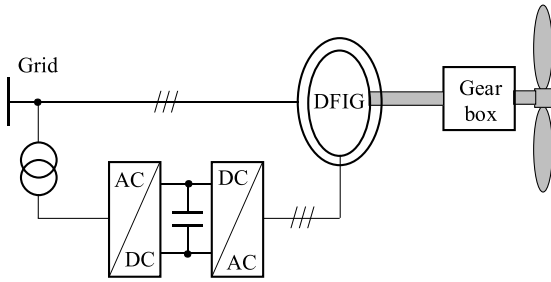
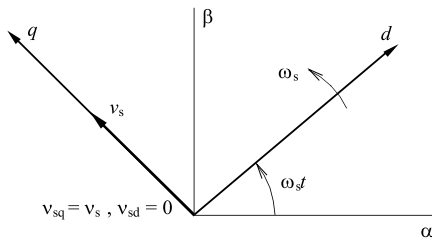


Fig. 1. DFIG wind turbine system


 Fig. 2. Choice of  $d$ - $q$  frame orientation

of fault is investigated. The effectiveness of the fuzzy logic controller is then compared with that of a PI controller. The validity of the controllers in restoring the wind farms normal operation after the clearance of fault is illustrated by the simulation results which are performed and analyzed under different fault conditions.

## 2 MATHEMATICAL MODEL OF THE DFIG

For analysis of control strategies, the mathematical model of doubly fed induction machine, in per unit notation with motor convention in  $d$ - $q$  reference frame is [13]

$$v_{sd} = r_s i_{sd} - \frac{\omega}{\omega_b} \psi_{sq} + \frac{1}{\omega_b} \frac{d\psi_{sd}}{dt}, \quad (1)$$

$$v_{sq} = r_s i_{sq} + \frac{\omega}{\omega_b} \psi_{sd} + \frac{1}{\omega_b} \frac{d\psi_{sq}}{dt}, \quad (2)$$

$$v_{rd} = r_r i_{rd} - \frac{\omega - \omega_r}{\omega_b} \psi_{rq} + \frac{1}{\omega_b} \frac{d\psi_{rd}}{dt}, \quad (3)$$

$$v_{rq} = r_r i_{rq} + \frac{\omega - \omega_r}{\omega_b} \psi_{rd} + \frac{1}{\omega_b} \frac{d\psi_{rq}}{dt}. \quad (4)$$

In these equations,  $\omega$  is the rotational speed of the  $d$ - $q$  reference frame (rad/sec), and it represents the grid frequency.  $\omega_b$  is the base speed which will be the systems nominal speed  $\omega_s$  (rad/s) and  $\omega_r$  is the electrical speed of the rotor (rad/s).  $v_s$  and  $v_r$  are the stator and rotor voltages (pu).  $i_s$  and  $i_r$  are the stator and rotor currents (pu).  $r_s$  and  $r_r$  are the stator and rotor resistances (pu).  $\Psi_s$  and  $\Psi_r$  are the stator and rotor magnetic fluxes linkage (pu).

The correlation between fluxes and currents is [14]

$$\psi_{sd} = \chi_{sd} i_{sd} + \chi_{md} i_{rd}, \quad (5)$$

$$\psi_{sq} = \chi_{sq} i_{sq} + \chi_{mq} i_{rq}, \quad (6)$$

$$\psi_{rd} = \chi_{rd} i_{rd} + \chi_{md} i_{sd}, \quad (7)$$

$$\psi_{rq} = \chi_{rq} i_{rq} + \chi_{mq} i_{sq} \quad (8)$$

where  $\chi_s$  and  $\chi_r$  are the stator and rotor leakage reactances (pu),  $\chi_m$  is the mutual magnetizing reactance (pu). The electromechanical torque  $T_{em}$  (pu) is given by

$$T_{em} = i_{sq} \psi_{sd} - i_{sd} \psi_{sq}. \quad (9)$$

In this paper, the  $d$ - $q$  frame is rotating at the synchronous speed *ie*  $\omega = \omega_s$ . The  $q$  axis is aligned with the stator voltage, as shown in Fig. 2. This implies that  $v_{sd} = 0$  and  $v_{sq} = v_s$ . This approach is useful for doubly fed machines where the control is performed by a means of the rotor voltage. The stator voltage is the grid voltage, which is approximately constant in a stable grid. The rotor voltage is referred to the same frame. It consists in general of two non-zero  $d$ - $q$  components. This  $d$ - $q$  frame orientation decouples the active power from reactive power and they can be controlled independently. The stator active power  $P_s$  and reactive power  $Q_s$  are expressed as follows

$$P_s = v_{sq} i_{sq}, \quad (10)$$

$$Q_s = v_{sq} i_{sd}. \quad (11)$$

## 3 WIND TURBINE MODEL

### 3.1 The aerodynamic model

The aerodynamic model of a wind turbine is determined by its power speed characteristics [15]. For a horizontal axis wind turbine, the mechanical power output that a turbine can produce is given by

$$P_m = \frac{1}{2} C_P(\lambda, \beta) \rho u^3 A \quad (12)$$

where  $\rho$  is the air density (kg/m<sup>3</sup>),  $u$  is the wind speed (m/s),  $A$  is the area covered by the rotor (m<sup>2</sup>), and  $C_p$  is the power coefficient which is a function of both tip speed ratio,  $\lambda$ , and blade pitch angle  $\beta$  (deg). In this work, the  $C_P$  equation is approximated using a non-linear function according to [16].

$$C_P(\lambda, \beta) = 0.22 \left( \frac{116}{\lambda_i} - 0.4\beta - 5 \right) e^{-\frac{12.5}{\lambda_i}} \quad (13)$$

where  $\lambda_i$  is given by

$$\frac{1}{\lambda_i} = \frac{1}{\lambda + 0.08\beta} - \frac{0.035}{\beta^3 + 1}. \quad (14)$$

The turbine power characteristics are illustrated as shown in Fig. 3. These characteristics are plotted at pitch angle  $\beta = 0$  (deg).

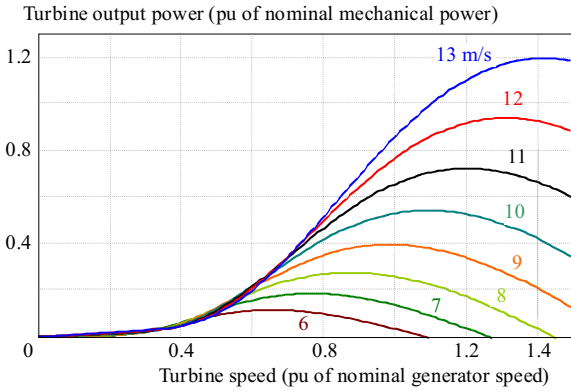


Fig. 3. The turbine power characteristics

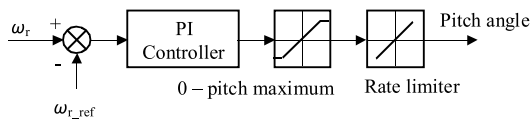


Fig. 4. The rotor speed control diagram

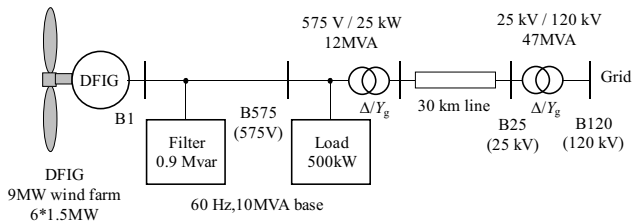


Fig. 5. The model system

### 3.2 Pitch angle controller

In this study, the conventional pitch angle controller shown in Fig. 4 is used. The minimum pitch angle  $\beta_{min}$  is  $0^\circ$  and the maximum pitch angle  $\beta_{max}$  is  $45^\circ$ . Accordingly, for a more realistic simulation, a rate limiter is implemented in the pitch controller model. In this paper the maximum pitch angle rate is set at 2 degrees/second. The purpose of using the pitch controller is to maintain the output power of wind generator at rated level by controlling the blade pitch angle of turbine blade when wind speed is over the rated speed.

## 4 WIND FARM MODEL SYSTEM

The power system model used for dynamic response of DFIG based wind farm is as shown in Fig. 5. Here, a 9 MW wind farm consisting of six 1.5 MW wind turbines connected to a 25 kV distribution system exports power to a 120 kV grid through a 30 km, 25 kV feeder. A 500 kW resistive load and a 0.9 Mvar (quality factor=50) are connected at the 575 V generation bus. This filter is used for reactive power compensation. The turbine power characteristics are illustrated as shown in Fig. 3. Wind

turbines using a doubly-fed induction generator consist of a wound rotor induction generator and an AC/DC/AC IGBT- based PWM converter. The switching frequency is chosen to be 1620 Hz. The stator winding is connected directly to the 60 Hz grid while the rotor is fed at variable frequency through the AC/DC/AC converter. The DFIG technology allows extracting maximum energy from the wind for low wind speeds by optimizing the turbine speed, while minimizing mechanical stresses on the turbine during gusts of wind. The optimum turbine speed producing maximum mechanical energy for a given wind speed is proportional to the wind speed. The data of wind turbines, DFIG, PWM converter, and DC link are illustrated in Appendix. The system base is 10 MVA.

## 5 ROTOR SIDE CONVERTER CONTROLLER

The stator of DFIG is connected directly to the grid. The rotor of DFIG is connected to the grid through AC/DC/AC frequency converter. The simulation program is carried out in a numerical simulation, using one of Matlab toolboxes, Simulink. All the system components are simulated using this program blocks.

The stator currents  $I_{abc-s}$ , the rotor currents  $I_{abc-r}$  and the grid converter currents  $I_{abc-grid-conv}$  are transformed into the  $d-q$  quantities  $I_{dq-s}$ ,  $I_{dq-r}$ , and  $I_{dq-grid-conv}$  respectively. The voltage of the bus  $B_1$  is  $V_{abc}$ . Three-phase phase locked loop (PLL) can be used to get the frequency of the voltage waveform and the angle theta ( $\theta = \omega t$ ). A torque controller is used to control the torque and maintains the speed  $\omega_r$  at certain constant value. The inputs of the torque controller are  $\omega_r$ ,  $I_{dq-s}$ ,  $I_{dq-r}$ ,  $I_{dq-grid-conv}$ , frequency, and  $V_{dqs}$ . The output of the torque controller is the  $d$ -axis desired rotor current  $I_{dr}^*$ . The torque controller consists of two cascaded blocks. The first block is called torque reference, which can be used to produce the command torque signal  $T_{com}$ . The second block is the torque regulator, which can be used to produce  $I_{dr}^*$ . Inside the torque reference block, the power losses of DFIG is subtracted from the input mechanical power of DFIG to obtain the reference electrical output power  $P_{ele.ref}$  of DFIG.  $P_{ele.ref}$  is divided by the generator speed  $\omega_r$  to get the torque command  $T_{com}$ . In the torque regulator, stator flux estimator is used to estimate the magnetic flux. The magnetic flux and  $T_{com}$  are used to get  $I_{dr}^*$ . The reactive power controller ( $Q$  regulator) is used to produce the  $q$ -axis desired rotor current  $I_{qr}^*$  where the  $Q_{ref}$  is compared with the actual  $Q$  of bus  $B_1$  and the reactive power error is used to produce  $I_{qr}^*$  via a PI controller. A current regulator is used to produce the reference voltages  $V_{dq}^*$ . These  $d-q$  voltages can be transformed into abc quantities to produce the control signals of the rotor converter. These control signals feed three phase pulse width modulation (PWM) generator to produce the firing pulses to the rotor converter.

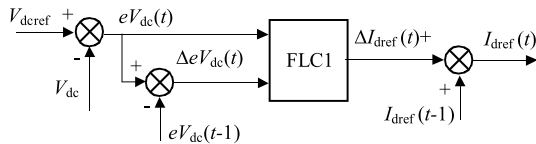


Fig. 6. The FLC1

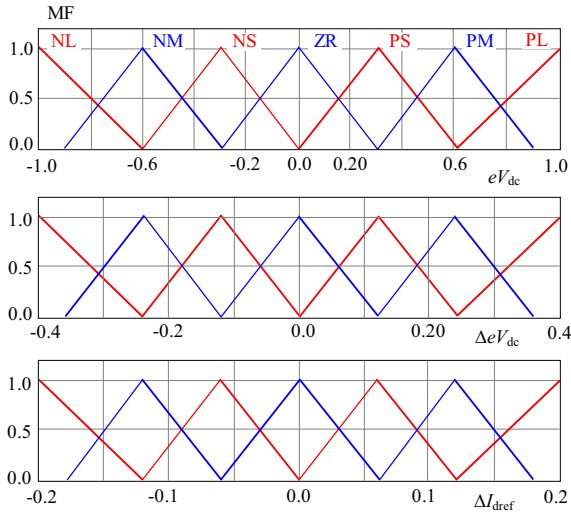


Fig. 7. The membership functions of FLC1

Table 1. The rules of FLC1

		$eV_{dc}$						
		NL	NM	NS	ZR	PS	PM	PL
$\Delta eV_{dc}$	NL	PL	PL	PM	PM	PS	PS	ZR
	NM	PL	PM	PM	PS	PS	ZR	NS
	NS	PM	PM	PS	PS	ZR	NS	NS
	ZR	PM	PS	PS	ZR	NS	NS	NM
	PS	PS	PS	ZR	NS	NS	NM	NM
	PM	PS	ZR	NS	NS	NM	NM	NL
	PL	ZR	NS	NS	NM	NM	NL	NL

### 6 GRID SIDE CONVERTER CONTROLLER

In the grid side converter controller, the voltage of bus  $B_1$   $V_{abc}$  and the grid converter currents  $I_{abc-grid-conv}$  are transformed into the  $d-q$  quantities  $V_{dq}$  and  $I_{dq}$  respectively. A dc bus voltage regulator is used to produce  $I_{dref}$ . The inputs of the dc bus voltage regulator are the reference dc bus voltage  $V_{dcref}$  and the actual value of dc bus voltage  $V_{dc}$ .  $V_{dc}$  is compared with  $V_{dcref}$  to yield the voltage error which feeds a PI controller to get  $I_{dref}$ . A current regulator is used to produce the reference voltages  $V_{dq}^*$ . These  $d-q$  voltages can be transformed into abc quantities to produce the control signals of the grid converter. These control signals feed three phase PWM generator to produce the firing pulses to the grid converter.

### 7 THE FUZZY LOGIC CONTROLLER (FLC)

For a good performance of DFIG based wind farm, four fuzzy logic controllers FLC1, FLC2, FLC3, and FLC4 are used. The PI controller in the dc bus voltage regulator is replaced by the FLC1. The PI controller in the reactive power regulator is replaced by the FLC2. The PI controllers in current regulators of rotor side converter controller and grid side converter controller are replaced by the FLC3 and FLC4 respectively.

In FLC1, the reference dc bus voltage  $V_{dcref}$  is compared with the actual voltage  $V_{dc}$  to obtain the voltage error  $eV_{dc}(t)$  as shown in Fig. 6. Also this error is compared with the previous error  $eV_{dc}(t-1)$  to get the change in error  $\Delta eV_{dc}(t)$ . The inputs of FLC1 are  $eV_{dc}(t)$  and  $\Delta eV_{dc}(t)$ . The output of the proposed controller is  $\Delta I_{dref}(t)$  which is added to the previous state of current  $I_{dref}(t-1)$  to obtain the reference current  $I_{dref}(t)$ . The others FLCs are based on the same approach as in FLC1.

The membership functions are defined off-line, and the values of the variables are selected according to the behavior of the variables observed during simulations. The selected fuzzy sets for FLC1 are shown in Fig. 7. The control rules of the FLC1 are represented by a set of chosen fuzzy rules. The designed fuzzy rules used in this work are given in Table 1. The fuzzy sets have been defined as: NL, negative large, NM, negative medium, NS, negative small, ZR, zero, PS, positive small, PM, positive medium and PL, positive large respectively.

### 7 SIMULATION RESULTS

In this study, the steady state operation of the DFIG and its dynamic response to voltage sag resulting from a remote fault on the 120 kV grid are observed. The wind speed is main tained constant at 10 m/s. The control system as stated above uses a torque controller in order to maintain the speed at 1.09 pu The reactive power produced by the wind turbine is regulated at 0 Mvar.

Two cases are taken into consideration according to the severity of the fault as described below.

#### 7.1 Case One

Initially the DFIG based wind farm produces 4.8 MW. This active power corresponds to the maximum mechanical turbine output for a 10 m/s wind speed ( $0.55 * 9 \text{ MW} = 4.95 \text{ MW}$ ) minus electrical and mechanical losses in the generator. The corresponding turbine speed is 1.09 pu of generator synchronous speed. The dc bus voltage is regulated at 1200 V and reactive power is kept at 0 Mvar. At  $t = 0.03 \text{ s}$ , the positive-sequence voltage suddenly drops to 0.8 pu causing an oscillation on both the dc bus voltage and the DFIG output power. During the voltage sag, the control system regulates dc bus voltage and reactive power at their set points (1200 V, 0 Mvar). The system recovers to the original state at  $t = 0.13 \text{ s}$ .

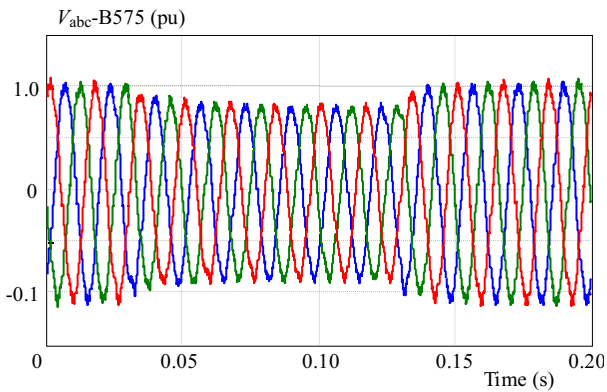


Fig. 8. The voltage  $V_{abc-B575}$  (pu)

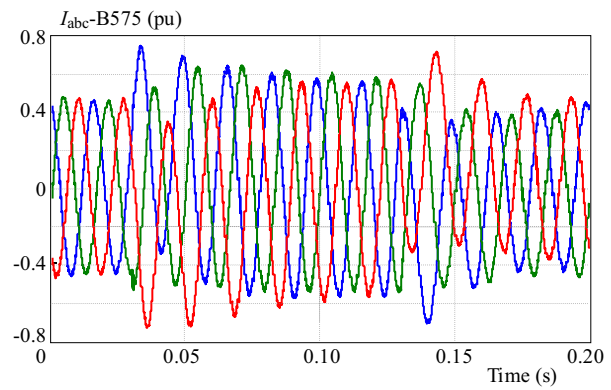


Fig. 9. The current  $I_{abc-B575}$  (pu)

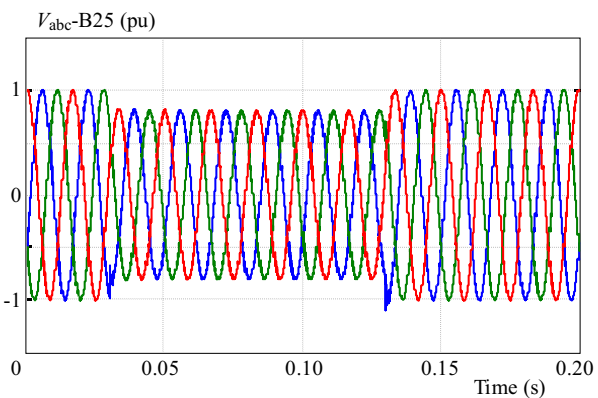


Fig. 10. The voltage  $V_{abc-B25}$  (pu)

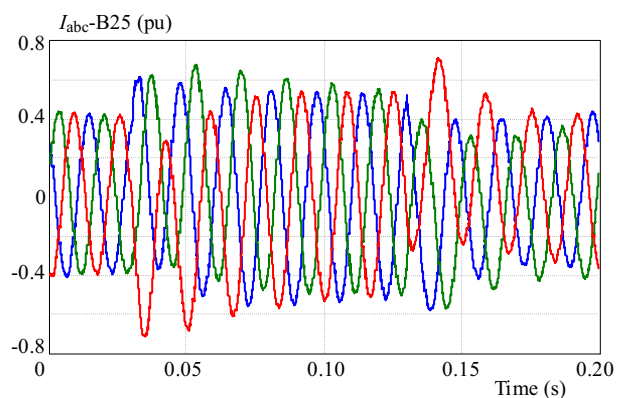


Fig. 11. The current  $I_{abc-B25}$  (pu)

Table 2. The optimal values of the PI controllers gains Pitch angle controller

Pitch angle controller	$k_p = 500, k_i = 20$
Reactive power controller	$k_p = 0.05, k_i = 5$
DC bus voltage controller	$k_p = 0.002, k_i = 0.05$
Grid side converter current controller	$k_p = 2.5, k_i = 500$
Rotor side converter current controller	$k_p = 0.3, k_i = 8$

Table 3. The optimal values of the PI controllers gains

Pitch angle controller	$k_p = 500, k_i = 20$
Reactive power controller	$k_p = 0.01, k_i = 5$
DC bus voltage controller	$k_p = 0.001, k_i = 0.02$
Grid side converter current controller	$k_p = 2.5, k_i = 400$
Rotor side converter current controller	$k_p = 0.3, k_i = 8$

The optimal values of the gains of the PI controllers are set as shown in Table 2. These PI controllers gains are optimized using the most commonly used Ziegler Nicholas method.

Figures 8–15 show the dynamic response of DFIG based wind farm under this fault conditions when provided with the proposed fuzzy logic controllers as compared with the PI controllers of optimal gains. By inspection of the dynamic response, it can be realized that the dynamic response of the DFIG based wind farm when provided with the fuzzy logic controllers is improved compared with that obtained when the DFIG based wind

farm is provided with the PI controllers. The response is fast with minimum overshoots. Moreover, the steady state error after the clearance of fault is rigorously reduced when the fuzzy logic controllers are used.

## 7.2 Case Two

The initial conditions of the DFIG based wind farm are the same as in case one. The DC voltage is regulated at 1200 V and the reactive power is kept at 0 Mvar. At  $t = 0.03$  s the positive-sequence voltage suddenly drops to 0.5 pu causing a very large oscillations on the DC bus voltage and on the DFIG output power. During the voltage drop, the control system regulates DC voltage and reactive power at their set points (1200 V, 0 Mvar). In this case, the controllers of DFIG based wind farm deal with a severe fault. Here, the main target of these controllers is to diminish the oscillations and also to improve the stability of the system.

The optimal values of the gains of the PI controllers are set as shown in Table 3.

Figures 16–23 show the dynamic response of the DFIG based wind farm under this fault conditions when provided with the proposed fuzzy logic controllers as compared with the PI controllers of optimal gains. It can be observed that during the voltage drop period and the instants after clearance of the fault, there are some little fluctuations in active and reactive power but the system

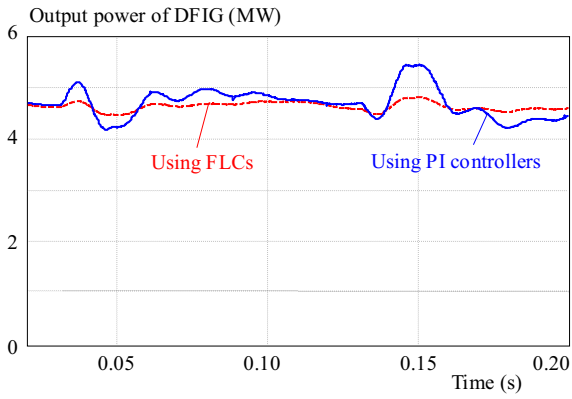


Fig. 12. The active output power of DFIG (MW)

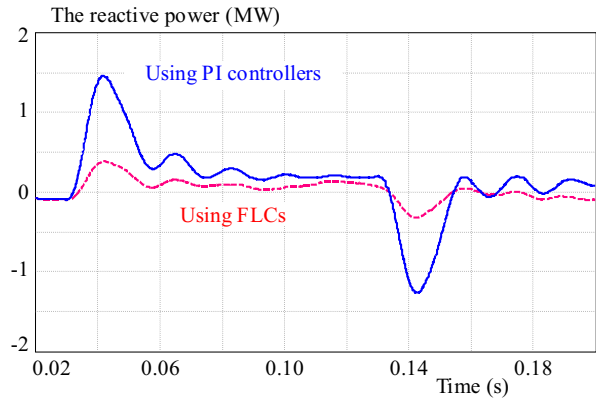


Fig. 13. The reactive power (Mvar)

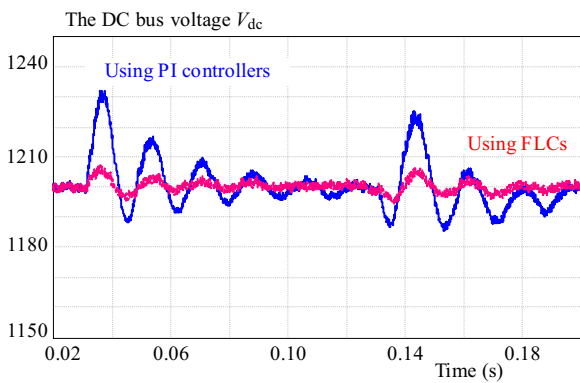


Fig. 14. The DC link voltage  $V_{dc}$

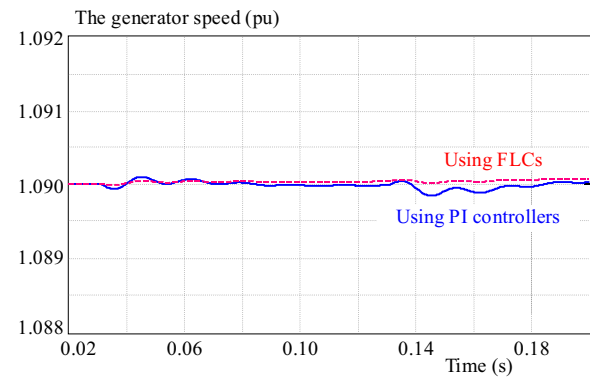


Fig. 15. The generator speed  $\omega_r$  (pu)

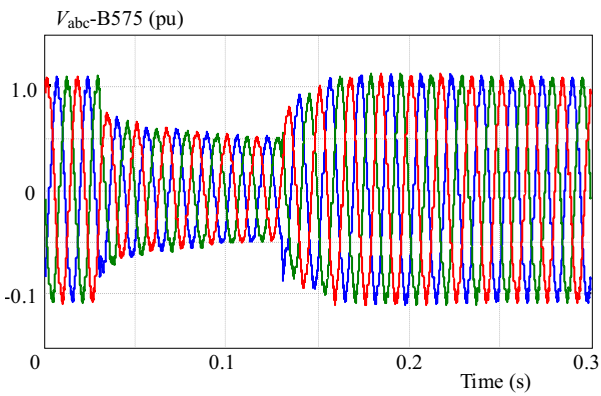


Fig. 16. The voltage  $V_{abc-B575}$  (pu)

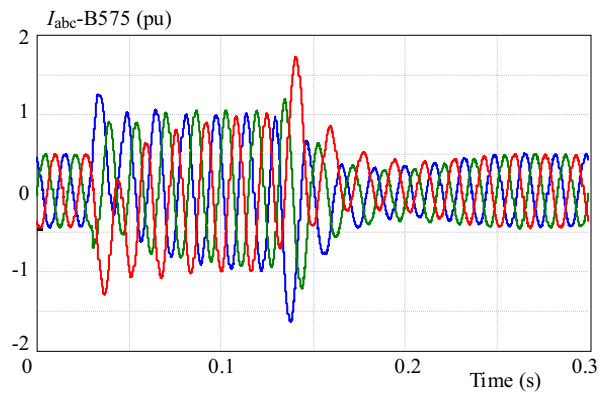


Fig. 17.  $I_{abc-B575}$  (pu)

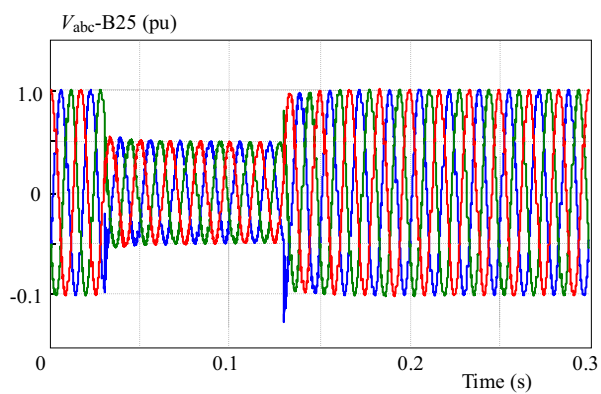


Fig. 18. The voltage  $V_{abc-B25}$  (pu)

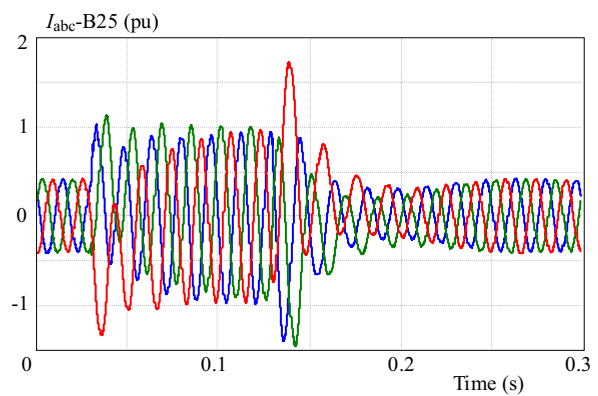


Fig. 19. The current  $I_{abc-B25}$  (pu)

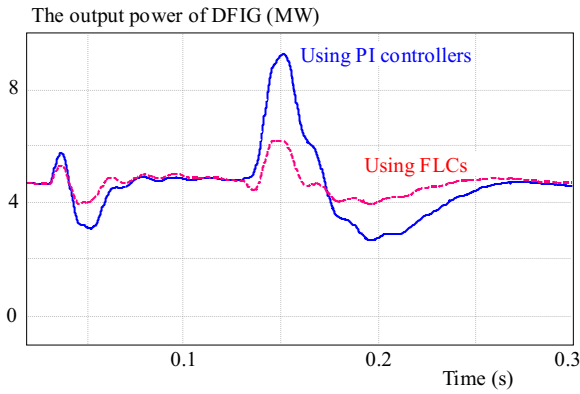


Fig. 20. The active output power of DFIG (MW)

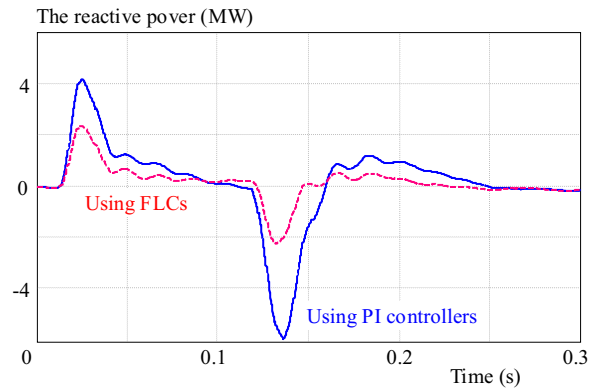


Fig. 21. The reactive power (Mvar)

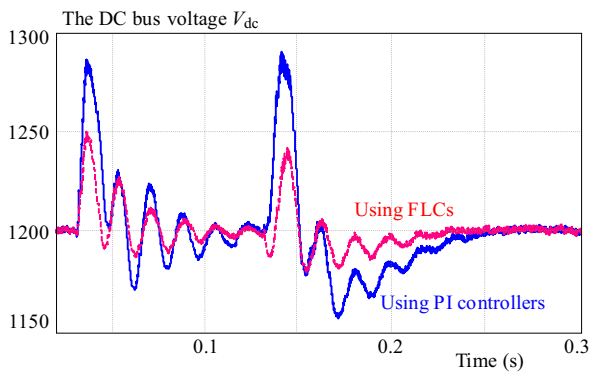


Fig. 22. The DC link voltage  $V_{dc}$

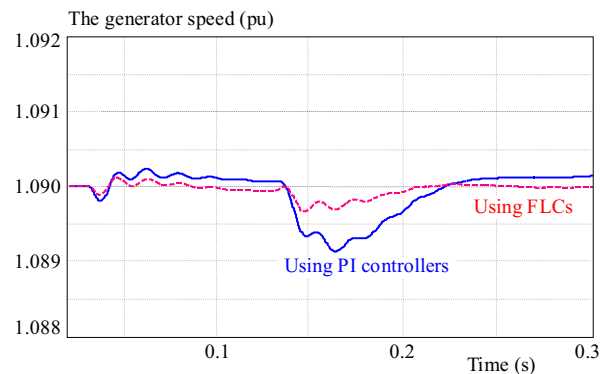


Fig. 23. The generator speed  $\omega_r$  (pu)

recovers to its good stability state. By inspection of the dynamic response, it can be realized that the dynamic response of the DFIG based wind farm when provided with the fuzzy logic controllers has maximum percentage overshoot lower than that experienced by the PI controllers. The fuzzy logic controllers improve the system damping after the first overshoot in compared with that of the PI controllers. It also yields a much faster response that allows the system to reach the steady state after 0.22 s, while in the PI technique; it reaches the steady state after 0.25 s.

### 9 CONCLUSION

This paper has presented a novel fuzzy logic controller to ensure dynamic response improvement of doubly-fed induction generator based wind farm under remote fault conditions. The fuzzy logic controller is found to enhance the transient stability of DFIG based wind farm during and after the clearance of the fault under different fault conditions. The dynamic response is found to be superior to that corresponding to the conventional PI controller. The proposed methodology is even suitable to other power systems related applications such as FACTS devices, voltage source converter based HVDC system and so on, especially in the cases where it is difficult to determine the suitable transfer function of a complex and larger system.

### APPENDIX

Doubly-fed induction generator data, PWM and DC link data and wind farm data.

Table 4. Doubly-fed induction generator data

The number of units	6
The nominal apparent power for each unit	1.666 MVA
The total apparent power ( $p_{nom}$ )	10 MVA
The nominal line-line voltage ( $V_{rms}$ )	575 V
The nominal frequency ( $f_{nom}$ )	60 Hz
The stator resistance ( $r_s$ )	0.00706 pu
The stator inductance ( $L_s$ )	0.171 pu
The rotor resistance ( $r_r$ )	0.005 pu
The rotor inductance ( $L_r$ )	0.156 pu
The mutual inductance ( $L_m$ )	2.9 pu
Number of pole pairs	3
Inertia constant ( $H$ )	5.04 s
Friction factor ( $F$ )	0.01 pu

Table 5. Wind farm data

Number of units	6
The nominal mechanical power of each unit ( $p_{mec}$ )	1.5 MW
The total mechanical power	9 MW
The base wind speed	11 m/s
The maximum power at base wind speed (pu of nominal mechanical power)	0.73 pu
Base rotational speed (pu of base generator speed)	1.2 pu

**Table 6.** PWM and DC link data

The PWM frequency	$27 * f_{nom}$
The nominal DC link Voltage $V_{dc}$	1200 V
The DC bus capacitor ( $C$ )	60000 ( $\mu F$ )

## Acknowledgement

This work was supported by Saudi Aramco Chair in Electrical Power, King Saud University, Riyadh, Saudi Arabia.

## REFERENCES

- [1] SUN, T.—CHEN, Z.—BLAABJERG, F.: Transient Analysis of Grid-Connected Wind Turbines with DFIG after an External Short-Circuit Fault, Nordic Wind Power Conference, vol. 1, March 2004.
- [2] MUYEEN, S. M.—TAKAHASHI, R.—MURATA, T.—TAMURA, J.: Transient Stability Enhancement of Variable Speed Wind Turbine Driven PMSG with Rectifier-Boost Converter-Inverter, in Proc. International Conference on Electrical Machines (ICEM), Sep 2008.
- [3] CAO, W.—HUANG, X.—FRENCH, I.—LU, B.: Simulation of a Site-Specific Doubly-Fed Induction Generator (DFIG) for Wind Turbine Applications, in Proc. International Conference on Electrical Machines (ICEM), Sep 2008.
- [4] POURBEIK, P.—KOESSLER, R. J.—DICKMANDER, D. L.—WONG, W.: Integration of Large Wind Farms into Utility Grids (Part 2 – Performance Issues), in Proc. IEEE PES Annual Meeting, vol. 3, 13-17 July 2003.
- [5] DATTA, R.—RANGANATHAN, V. T.: Variable-Speed Wind Power Generation using Doubly Fed Wound Rotor Induction Machine – a Comparison with Alternative Schemes, IEEE Transactions on Energy Conversion **17** No. 3 (Sep 2002), 414–421.
- [6] NIIRANEN, J.: Voltage Dip Ride through of a Doubly-Fed Generator Equipped with an Active Crowbar, Nordic Wind Power Conference, vol. 1, March 2004.
- [7] SLOOTWEG, J. G.—de HAAN, S. W. H.—POLINDER, H.—KLING, W. L.: General Model for Representing Variable Speed Wind Turbines in Power System Dynamics Simulations, IEEE Transactions on Power Systems **18** No. 1 (Feb 2003), 144–151.
- [8] HASANIEN, H. M.—MUYEEN, S. M.: Design Optimization of Controller Parameters used in Variable Speed Wind Energy Conversion System by Genetic Algorithms, IEEE Transactions on Sustainable Energy **3** No. 2 (Apr 2012), 200–208.
- [9] HASANIEN, H. M.—MUYEEN, S. M.: Speed Control of Grid-Connected Switched Reluctance Generator Driven by Variable Speed Wind Turbine using Adaptive Neural Network Controller, Electric Power Systems Research **84** No. 1 (March 2012), 206–213, Elsevier.
- [10] MUYEEN, S. M.—HASANIEN, H. M.—TAMURA, J.: Reduction of Frequency Fluctuation for Wind Farm Connected Power Systems by an Adaptive Artificial Neural Network Controlled Energy Capacitor System, IET Renewable Power Generation **6** No. 4 (July 2012), 226–235.
- [11] de ALMEIDA, R. G.—LOPES, P. J. A.—BARREIROS, J. A. L.: Improving Power System Dynamic Behavior through Doubly Fed Induction Machine Controlled by Static Converter using Fuzzy Control, IEEE Transactions on Power Systems **19** No. 4 (Nov 2004), 1942–1950.
- [12] Release 2008a, MATLAB, The Math Works press, March 2008.
- [13] SOENS, J.—DRIESEN, J.—BELMANS, R.: A Comprehensive Model of a Doubly Fed Induction Generator for Dynamic Simulations and Power System Studies, in Proc. International Conference on Renewable Energies and Power Quality, Vigo, Spain, April 2003.
- [14] KRAUSE, P. C.—WASYNCZUK, O.—SUDHOFF, S. D.: Analysis of Electric Machinery, IEEE Press, New York, 1995, pp. 172–175.
- [15] JOHNSON, G. L.: Wind Energy Systems, reference book, Manhattan, KS, 2001.
- [16] HEIER, S.: Grid Integration of Wind Energy Conversion Systems, John Wiley & Sons Ltd., 1998.

Received 8 January 2012

**Hany M. Hasanien** (M'09-SM'11). He was born in Cairo, Egypt on May 20, 1976. He received his BSc, MSc and PhD degrees in Electrical Engineering from Ain Shams University, Faculty of Engineering, Cairo, Egypt, in 1999, 2004, and 2007 respectively. He is an Associate Professor at the Electrical Power and Machines Dept., Faculty of Engineering, Ain Shams University. Currently, he is on leave as an Assistant Professor at the Electrical Engineering Dept., College of Engineering, King Saud University. His research interests include electrical machines design, modern control techniques, electrical drives, and artificial intelligence applications on electrical machines and renewable energy systems. Dr. Hasanien is a Senior member of the Institution of Electrical and Electronics Engineers (IEEE) and also of Power & Energy Society (PES). His biography has been included in Marquis Whos Who in the world for its 28th edition, 2011.

**Essam Al-Ammar** was born in Riyadh, Saudi Arabia. He received his BS degree (honor) in Electrical Engineering from King Saud University in 1997. From 1997-1999, he worked as a Power/software engineer at Lucent Technologies in Riyadh. He worked as an Instructor at King Saud University between 1999-2000. In 2003, he received his MS degree from University of Alabama, Tuscaloosa, AL, and Ph.D. degree from Arizona State University in 2007. He is now an associate professor in Electrical Engineering Department, King Saud University, Riyadh, Saudi Arabia. Since Nov. 2008, he has appointed as advisor at Ministry of Water and Electricity (MOWE), and become as coordinator of Saudi Aramco Chair in electrical power. He worked as energy consultant at Riyadh Techno Valley (RTV), between Oct. 2009 and Oct. 2011. His current research and academic interests include high voltage engineering, power system transmission, distribution and protection. Solar and wind energies are part of his research interest too. He is a member of IEEE since 2007 and Saudi Engineering Committee since 1997. He involves in different technical committees, and has authored more than 45 technical papers in different power aspects.